

MARIS: Referring Image Segmentation via Mutual-Aware Attention Features

Mengxi Zhang, Yiming Liu, Xiangjun Yin, Huanjing Yue, Jingyu Yang *

Abstract

Referring image segmentation (RIS) aims to segment a particular region based on a language expression prompt. Existing methods incorporate linguistic features into visual features and obtain multi-modal features for mask decoding. However, these methods may segment the visually salient entity instead of the correct referring region, as the multi-modal features are dominated by the abundant visual context. In this paper, we propose MARIS, a referring image segmentation method that leverages the Segment Anything Model (SAM) and introduces a mutual-aware attention mechanism to enhance the cross-modal fusion via two parallel branches. Specifically, our mutual-aware attention mechanism consists of Vision-Guided Attention and Language-Guided Attention, which bidirectionally model the relationship between visual and linguistic features. Correspondingly, we design a Mask Decoder to enable explicit linguistic guidance for more consistent segmentation with the language expression. To this end, a multi-modal query token is proposed to integrate linguistic information and interact with visual information simultaneously. Extensive experiments on three benchmark datasets show that our method outperforms the state-of-the-art RIS methods. Our code will be publicly available.

Introduction

Referring image segmentation (Hu, Rohrbach, and Darrell 2016) (RIS) is a fundamental and challenging multi-modal task, which involves both vision-language understanding (Li et al. 2022a) and instance segmentation (He et al. 2017). The target of RIS is to locate particular regions according to the given query in natural language. It has great potential in many applications, *e.g.*, human-machine interaction and interactive image segmentation.

Existing RIS methods (Hu et al. 2020; Ding et al. 2022; Liu, Ding, and Jiang 2023) introduce various fusion methods to obtain multi-modal features. Then, these features are sent into a mask decoder to predict the segmentation mask.

*Mengxi Zhang, Xiangjun Yin, Huanjing Yue, Jingyu Yang (corresponding author) are with the School of Electrical and Information Engineering, Tianjin University, Tianjin 300072, China (e-mail: mengxizhang@tju.edu.cn; yjy@tju.edu.cn; yinxianjun@tju.edu.cn; huanjing.yue@tju.edu.cn). Copyright © 2024, Association for the Advancement of Artificial Intelligence (www.aaai.org). All rights reserved.

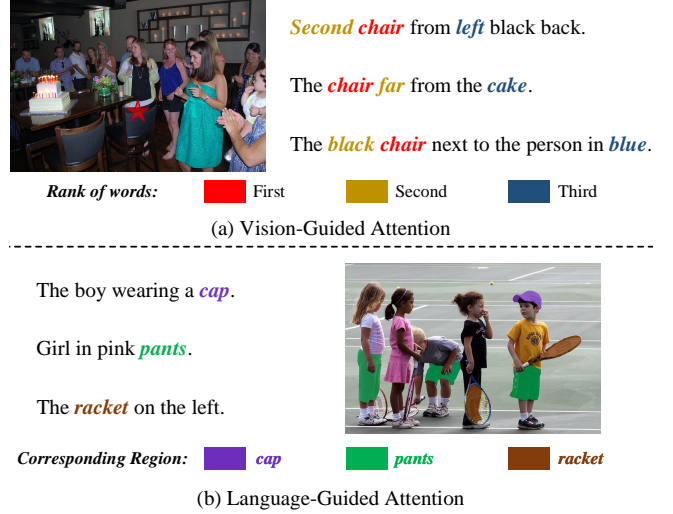


Figure 1: The illustration of Vision-Guided Attention (a) and Language-Guided Attention (b). For Vision-Guided Attention, we list the three most informative words for the image region symbolized by a red pentangle. For Language-Guided Attention, the most corresponding regions for each word, *e.g.*, ‘cap’, ‘pants’, and ‘racket’, are denoted by different colors. Previous RIS methods only consider Vision-Guided Attention to fuse visual and linguistic features, but none of these methods introduce Language-Guided Attention to generate vision-aware linguistic features and explicitly use them in the mask decoder.

Despite significant advancements in RIS, there are still several limitations. First, current methods (Ding et al. 2022; Liu, Ding, and Jiang 2023) utilize the unidirectional attention mechanism to fuse features from different modalities. However, they only consider the linguistic guidance for visual features but ignore the visual guidance for linguistic features. Unlike the unidirectional attention mechanism, BRINet (Hu et al. 2020) adopts both visual and linguistic guidance in a serial bidirectional way. Nevertheless, due to the serial manner, it only implicitly generates vision-aware linguistic features in the fusion model but does not explicitly use these features in the mask decoder. Second, existing methods use a mask decoder to generate the final segmen-



Figure 2: Segmentation masks generated by our method (c) and other methods, including directly using SAM (d), CRIS (Wang et al. 2022) (e), and ReLA (Liu, Ding, and Jiang 2023) (f). Directly using SAM means training the SAM decoder only. We provide more examples in the supplementary material.

tation mask from the multi-modal features. However, since multi-modal features are produced by integrating linguistic properties into visual features, they still contain a lot of visual properties. Without explicit linguistic guidance, the mask decoder focuses on the most visually salient entities but ignores linguistic consistency. Moreover, existing methods typically fine-tune the encoders to adapt them for the dataset of RIS. However, this strategy shrinks the generalization ability of encoders pre-trained on a large-scale dataset.

In this paper, we propose a novel method that utilizes the mutual-aware attention mechanism and transfers the knowledge of Segment Anything Model (SAM) (Kirillov et al. 2023) into RIS. First, we introduce the Mutual-Aware Attention block to bidirectionally model the relationship between visual and linguistic features. The Mutual-Aware Attention block consists of two parallel branches: Vision-Guided Attention and Language-Guided Attention. As shown in Fig. 1, Vision-Guided Attention assigns different weights to each word in the expression for each image region (such as the red pentangle) and produces language-aware visual features. Similarly, Language-Guided Attention explores the corresponding image region for the word, *e.g.*, ‘cap’, ‘pants’, ‘racket’, and generates vision-aware linguistic features. We consider language-aware visual features and vision-aware linguistic features as the mutual-aware attention features of our method. Second, we design a Mask Decoder to enable explicit linguistic guidance. Specifically, we introduce a multi-modal query token to integrate visual and linguistic properties, which helps to segment the correct referring region. Finally, we freeze the image encoder of SAM to preserve its generalization ability. To transfer the knowledge of SAM into RIS, we introduce a Feature Enhancement module to integrate global and local visual features.

We demonstrate the results of our method and other methods in Fig. 2. To our knowledge, our work is the first to transfer the powerful knowledge of SAM into RIS. To be summarized, our contributions are listed as follows:

- We propose a referring image segmentation method called MARIS, which leverages the powerful knowledge of SAM and uses the mutual-aware attention mechanism to

model the relationship between visual and linguistic features bidirectionally.

- We introduce a Mutual-Aware Attention block to produce language-aware visual features and vision-aware linguistic features by weighting each word of the sentence and each region of visual features.

- We design a Mask Decoder to utilize explicit linguistic guidance and get a segmentation mask consistent with the language expression. Besides, we introduce a multi-modal query token to integrate visual and linguistic properties.

- The proposed approach achieves new state-of-the-art performance on the three widely used RIS datasets, including RefCOCO, RefCOCO+, and G-Ref. Additionally, our method exhibits excellent generalization capabilities.

Related Work

Referring Image Segmentation

Referring image segmentation (Hu, Rohrbach, and Darrell 2016) aims to segment a particular region according to the natural language expression. Early approaches (Yu et al. 2016; Liu et al. 2017; Yu et al. 2018; Liu et al. 2019; Luo et al. 2020) concatenate visual and linguistic features to produce multi-modal features, which are fed into the fully convolutional network for segmentation generation. Yu et al. (Yu et al. 2018) proposed a two-stage method that first generates masks by Mask R-CNN (He et al. 2017), and then selected the target mask with linguistic prompt. Besides, MCN (Luo et al. 2020) presented a multi-task framework to jointly optimize two related tasks, *i.e.*, referring expression comprehension and segmentation.

As the attention mechanism (Vaswani et al. 2017; Wang et al. 2018) achieved great success in various fields, it has been exploited in the field of RIS (Shi et al. 2018; Ye et al. 2019; Hu et al. 2020; Jing et al. 2021). Later, some methods (Yang et al. 2022; Kim et al. 2022; Ding et al. 2022) adopt the transformer-based architectures. VLT (Ding et al. 2022) introduces a Vision-Language Transformer to enhance deep interactions among multi-modal features. More recently, CRIS (Wang et al. 2022) utilized CLIP (Radford et al. 2021) as the image and text encoder and transferred the

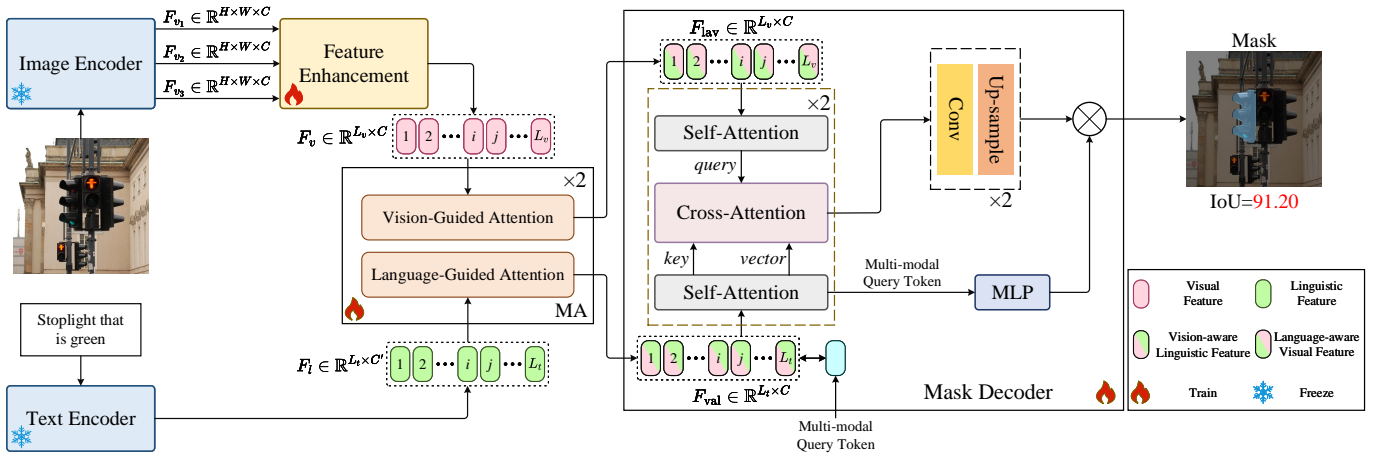


Figure 3: The overview of MARIS. For an input image, the image encoder extracts shallow/middle/deep visual features ($F_{v_1}, F_{v_2}, F_{v_3}$). For the language expression, the text encoder generates linguistic features (F_l). Then these features are sent into the Feature Enhancement module and obtain enhanced visual features (F_v). Subsequently, Mutual-Aware Attention (MA) blocks receive enhanced visual features and linguistic features as inputs to get mutual-aware attention features. After that, the Mask Decoder utilizes a multi-modal query token and mutual-aware attention features to get the final segmentation mask.

knowledge of CLIP for text-to-pixel alignment. ReLA (Liu, Ding, and Jiang 2023) introduced a new task called generalized referring expression segmentation, which enables expressions to indicate the existence of target objects. However, these methods fail to produce and explicitly utilize vision-aware linguistic features in the mask decoder.

Attention Mechanism

Attention mechanism has been widely used in various multi-modal tasks. In (Li et al. 2020; Zhou et al. 2020), Transformer schemes are used to exploit the long-range dependencies between visual features and linguistic features. Besides, the Transformer-decoder based architectures (Li et al. 2021, 2023) are also used to fuse the visual and linguistic features. For example, BLIP-2 (Li et al. 2023) builds a Q-former based on the cross-attention mechanism to assemble visual and linguistic information by a set of learned queries. Later, GLIP (Li et al. 2022a) introduces bidirectional cross-attention to obtain multi-modal features. Yang et al. (Yang et al. 2023) build a Trajectory to Word attention for video-language tasks. In this paper, we propose a Mutual-Aware Attention scheme to generate language-aware visual features and vision-aware linguistic features, where the latter guides the former to generate an accurate mask in the Mask Decoder.

Powerful Foundation Models in Computer Vision

Foundation models are trained on broad data and can be adapted (*e.g.*, fine-tuned) to a wide range of downstream tasks. In recent years, some vision transformers (Dosovitskiy et al. 2020; Liu et al. 2021) achieved state-of-the-art performance on various tasks, including image classification, semantic/instance segmentation, and object detection. Due to great efforts made on large-scale datasets, recent foundation models (Radford et al. 2021; Kirillov

et al. 2023) are equipped with more powerful feature representations. Benefiting from 400 million image-text pairs, CLIP (Radford et al. 2021) achieved strong zero-shot ability on many visual tasks. Some researchers utilize the knowledge of CLIP for different tasks, including semantic segmentation (Xu et al. 2022), object detection (Gu et al. 2021; Li et al. 2022a), and referring image segmentation (Wang et al. 2022). Recently, Meta released SAM, the first segmentation foundation model trained on more than 1 billion masks, and achieved remarkable performance on interactive segmentation. In this paper, we first propose a novel method that leverages the powerful knowledge of SAM in the field of RIS. Besides, we design the Mutual-Aware Attention block and the Mask Decoder to get an accurate segmentation mask.

Methodology

The overall architecture of MARIS is shown in Fig. 3. Firstly, the input image and language expression are projected into the visual ($F_{v_1}, F_{v_2}, F_{v_3}$) and linguistic (F_l) feature spaces via a pre-trained image encoder (Kirillov et al. 2023) and a text encoder (Radford et al. 2021), respectively. Note that the parameters of the image and text encoder are frozen. Secondly, we design a Feature Enhancement (FE) module, which fuses features from different layers of the image encoder and obtains enhanced visual features (F_v). Thirdly, enhanced visual features (F_v) and linguistic features (F_l) are fed into the Mutual-Aware Attention (MA) block to obtain mutual-aware attention features. Finally, we introduce the Mask Decoder (DE) with a single multi-modal query token to utilize explicit linguistic guidance and produce a language-consistent mask. We will describe the details of these steps in the following subsections.

Image Encoder and Text Encoder

The image encoder of SAM (Kirillov et al. 2023), a ViT-based backbone, takes images of size 1024×1024 as inputs and generates visual features of spatial size 64×64 . In particular, SAM uses a ViT-H with 14×14 windows and four plain global attention blocks. For an input image, we utilize visual features from 2nd~4th global attention blocks, which are defined as shallow layer features $F_{v_1} \in \mathbb{R}^{H \times W \times C}$, middle layer features $F_{v_2} \in \mathbb{R}^{H \times W \times C}$ and deep layer features $F_{v_3} \in \mathbb{R}^{H \times W \times C}$. Here, H and W are the height and width of the feature map, respectively, and C denotes the channel size of visual features.

For the language expression, we adopt a text encoder pretrained by (Radford et al. 2021) and obtain linguistic features $F_l \in \mathbb{R}^{L_t \times C'}$. Here, L_t denotes the length of linguistic features. Accordingly, C' is the channel size of linguistic features.

To preserve the generalization capability of the image and text encoder and save computational resources, we freeze the parameters of these encoders, which also prevents catastrophic forgetting (Toneva et al. 2018).

Feature Enhancement

To generate an accurate segmentation mask for the causal language expression, it is necessary to focus on both global semantic information and local grained details. For the image encoder of SAM, features from the deep layer and shallow layer contain accurate global features and abundant local features, respectively. Based on this consideration, we first fuse the shallow layer feature F_{v_1} and the middle layer feature F_{v_2} as follows.

$$\hat{F} = \text{CBA}([\text{MLP}(F_{v_1}), \text{MLP}(F_{v_2})]), \quad (1)$$

where \hat{F} denotes the early enhanced feature. $\text{CBA}(\cdot)$ is sequential operations, including convolution layers with 3×3 kernels, a batch-normalization layer, and GeLU activation function. $\text{MLP}(\cdot)$ represents the Multi-Layer Perceptron (MLP) layer. $[\cdot, \cdot]$ is the concatenation operation.

Subsequently, we fuse the early enhanced feature \hat{F} and the deep layer feature F_{v_3} to obtain the final enhanced visual feature,

$$F_v = \text{CBA}([\text{MLP}(\hat{F}), \text{MLP}(F_{v_3})]), \quad (2)$$

where $F_v \in \mathbb{R}^{H \times W \times C}$ is the final enhanced visual feature. Then the feature map is flattened into a 2-D vector $F_v \in \mathbb{R}^{L_v \times C}$, where L_v is equal to $H \times W$.

Mutual-Aware Attention

After obtaining visual and linguistic features, the first step is to fuse these features. Existing methods (Kim et al. 2022; Ding et al. 2022) propose different strategies to get multi-modal features. However, these methods only assign different weights to each word in the expression but treat each image region equally. BRINet (Hu et al. 2020) adopts a serial bidirectional design to utilize both visual and linguistic guidance. However, the serial design fails to utilize vision-aware linguistic features explicitly. To address these issues,

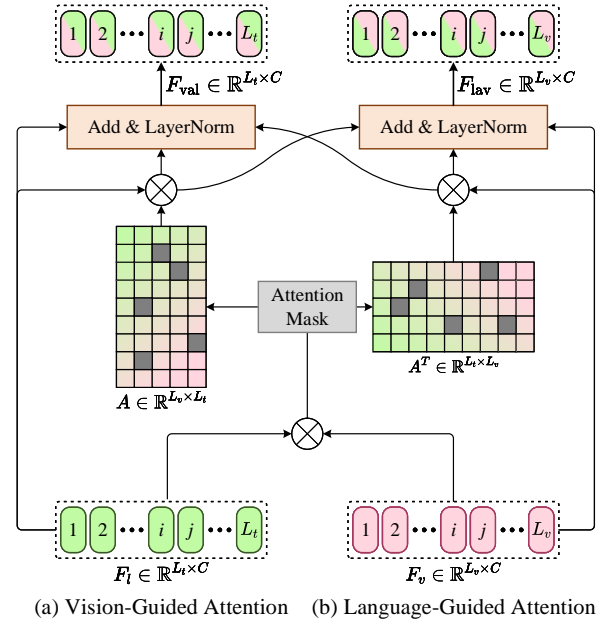


Figure 4: The architecture of Mutual-Aware Attention block. The left part (a) is the Vision-Guided Attention branch, and the right part (b) is the Language-Guided Attention branch. A and A^T denote the attention weights. \otimes symbolizes the matmul product operation.

we propose the Mutual-Aware Attention block, which consists of two parallel branches. Specifically, the first branch is Vision-Guided Attention, which weights different words for each pixel of visual features. Accordingly, the second branch is Language-Guided Attention, which weights different image regions for each word of the sentence. The architecture of Mutual-Aware Attention is shown in Fig. 4.

First, we model the correlation between linguistic features and visual features as follows,

$$\begin{aligned} Z_v &= F_v W_v, Z_l = F_l W_l, \\ A &= \text{Softmax}(Z_v Z_l^T + \mathcal{M}) \end{aligned} \quad (3)$$

where $A \in \mathbb{R}^{L_v \times L_t}$ is the attention weight. W_v and W_l are learnable matrices of size $C \times C$ and $C' \times C$, which aim to transform F_v and F_l into the same feature dimension. \mathcal{M} is the attention mask, which is calculated by,

$$\mathcal{M}(i, j) = \begin{cases} 0 & \text{if } M(i, j) < \tau \\ -\infty & \text{otherwise} \end{cases}, \quad (4)$$

where $M = 1/(1 + e^{-Z_v Z_l^T})$ denotes the relevant scores between visual and linguistic features. τ is the threshold, and its value will be discussed in the supplementary material. Through the attention mask \mathcal{M} , we alleviate the interference from irrelevant pairs in visual and linguistic features.

After that, we obtain mutual-aware attention features, including language-aware visual features $F_{lav} \in \mathbb{R}^{L_v \times C}$ and vision-aware linguistic features $F_{val} \in \mathbb{R}^{L_t \times C}$ as follows,

$$\begin{aligned} F_{lav} &= \text{LayerNorm}(A Z_l + Z_v), \\ F_{val} &= \text{LayerNorm}(A^T Z_v + Z_l). \end{aligned} \quad (5)$$

where $\text{LayerNorm}(\cdot)$ denotes the Layer Normalization.

We use two sequential Mutual-Aware Attention blocks in our implementation, and the ablation in terms of the number of Mutual-Aware Attention blocks will be discussed in the supplementary material.

Mask Decoder

The mutual-aware attention features are fed into the mask decoder to obtain the final mask. Since the multi-modal features contain excessive visual properties, the mask decoder is likely to segment visual-dominant entities without explicit linguistic guidance. To enable explicit linguistic guidance, we build a Mask Decoder based on the mask classification framework (Carion et al. 2020; Cheng et al. 2022). Specifically, we only use a single multi-modal query token with random initialization. Different from DETR/Mask2former, we combine the multi-modal query token with vision-aware linguistic features as the input of the decoder. Such a design enables the multi-modal query token to integrate linguistic information and interact with visual features, thus getting a consistent segmentation with the language expression.

To this end, language-aware visual feature F_{lav} is first fed into a multi-head self-attention layer to extract powerful contextual information.

$$\hat{F}_{\text{lav}} = \text{MHSA}(F_{\text{lav}}) + F_{\text{lav}}, \quad (6)$$

where $\text{MHSA}(\cdot)$ is the multi-head self-attention layer.

Then, the multi-modal query token $F_m \in \mathbb{R}^{1 \times C}$ along with $F_{\text{val}} \in \mathbb{R}^{L_t \times C}$ are sent to a multi-head self-attention layer to aggregate the vision-aware linguistic feature. Let $F_c := [F_m, F_{\text{val}}]$, The aggregation is formulated as

$$\hat{F}_c := [\hat{F}_m, \hat{F}_{\text{val}}] = \text{MHSA}(F_c) + F_c, \quad (7)$$

where \hat{F}_c denotes the evolved feature concatenating the evolved versions of vision-aware linguistic feature \hat{F}_{val} and multi-modal query token \hat{F}_m .

Subsequently, we perform interaction between \hat{F}_{lav} and \hat{F}_c , obtaining the evolved language-aware visual feature \bar{F}_{lav} via a multi-head cross-attention layer as follows.

$$\bar{F}_{\text{lav}} = \text{MHCA}(\hat{F}_{\text{lav}}, \hat{F}_c) + \hat{F}_{\text{lav}}. \quad (8)$$

where $\text{MHCA}(\cdot)$ is the multi-head cross-attention layer.

The next decoder block takes evolved language-aware visual feature \bar{F}_{lav} and evolved concatenated feature \hat{F}_c from the previous layer as inputs.

After that, the evolved language-aware visual feature \bar{F}_{lav} is upsampled by two sequential blocks. Each consists of a convolutional layer and an upsample operation. We extract the evolved multi-modal query token \hat{F}_m from the evolved concatenated feature \hat{F}_c , and send it to a MLP layer. Finally, we multiply the output of MLP with upsampled visual features to generate the segmentation mask.

Losses

In the training process, we adopt the linear combination of focal loss (Lin et al. 2017) and dice loss (Milletari, Navab, and Ahmadi 2016) formulated as follows.

$$\mathcal{L} = \mathcal{L}_f + \mathcal{L}_d, \quad (9)$$

where \mathcal{L}_f and \mathcal{L}_d are focal loss and dice loss, respectively.

Experiments

Datasets

We conduct experiments on three widely used datasets, including RefCOCO & RefCOCO+ (Kazemzadeh et al. 2014), and G-Ref (Mao et al. 2016). The images of these three datasets are from MSCOCO (Lin et al. 2014), but are annotated with language expressions with different styles. Expressions of RefCOCO/RefCOCO+ have an average length of 3.61/3.53. Compared with RefCOCO, expressions about absolute locations, *e.g.*, left/right, are forbidden in RefCOCO+. G-Ref has a longer average length (8.4 words). Following previous works, we evaluate both RefCOCO and RefCOCO+ in three subsets: validation, testA, and testB. For G-Ref, we leverage both partitions of UMD and Google for the evaluation.

Metrics

Following previous works (Ding et al. 2022; Liu, Ding, and Jiang 2023), we utilize two metrics in our experiments, including mask Intersection-over-Union (IoU) score and Precision with thresholds ($\text{Pr}@X$). Specifically, IoU scores reveal the predicted mask quality by calculating intersection regions over union regions between the predicted mask and the ground truth across all testing samples. Besides, $\text{Pr}@X$ denotes the ratio of predicted masks with IoU scores higher than the threshold $X \in \{70, 80, 90\}$. Implementation details are reported in the supplementary material. For example, $\text{Pr}@70$ denotes the location ability of the model, while $\text{Pr}@90$ shows the ability to generate a high-quality mask.

Comparison With State-of-the-art Methods

We compare the proposed MARIS with previous state-of-the-art (SOTA) methods on the three most widely used benchmarks, *i.e.*, RefCOCO, RefCOCO+, and G-Ref. Quantitative results are shown in Tab. 1.

Our method achieves significant improvements over the second-best SOTA method, MCRES (Xu et al. 2023), on the RefCOCO dataset. Specifically, our method outperforms MCRES by 1.28%, 1.94%, and 1.00% on the val, testA, and testB split, respectively. These results demonstrate the effectiveness of our framework for the RIS task.

On the RefCOCO+ dataset, our MARIS improves over ReLA (Liu, Ding, and Jiang 2023) on the val and testA splits by 0.33% and 1.08%, respectively. However, we observe a slight performance drop of 0.32% on the testB split compared to ReLA. A possible reason is that the frozen text encoder gets sub-optimal linguistic feature representation for language expression without absolute locations. When the test set (*i.e.*, testB split) contains images with multiple objects that are hard to be distinguished without absolute locations, our method exhibits inferior performance.

Finally, on another more complex G-Ref dataset, our method achieves an IoU improvement of 0.48%, 0.38%, and 1.98% on the val (U), test (U), and val (G) split, respectively. This improvement indicates that our method is also competitive for long and causal language expressions. Besides, we also demonstrate the ratio of predicted masks with IoU

Table 1: Comparisons with previous state-of-the-art methods in terms of IoU. U: UMD split; G: Google split.

Methods	RefCOCO			RefCOCO+			G-Ref		
	val	testA	testB	val	testA	testB	val (U)	test (U)	val (G)
SAM (ICCV'23)	57.23	58.71	56.34	44.95	50.35	41.38	47.87	49.31	46.23
ReSTR (CVPR'22)	67.22	69.30	64.45	55.78	60.44	48.27	-	-	54.48
CRIS (CVPR'22)	70.47	73.18	66.10	62.27	68.08	53.68	59.87	60.36	-
RefTR (NIPS'21)	70.56	73.49	66.57	61.08	64.69	52.73	58.73	58.51	-
LAVT (CVPR'22)	72.73	75.82	68.79	62.14	68.38	55.10	61.24	62.09	60.50
VLT (TPAMI'22)	72.96	75.96	69.60	63.53	68.43	56.92	63.49	66.22	62.80
ReLA (CVPR'22)	73.82	76.48	70.18	66.04	71.02	57.65	65.00	65.97	62.70
MCRES (CVPR'23)	74.92	76.98	70.84	64.32	69.68	56.64	63.51	64.90	61.63
MARIS (Ours)	76.20	78.92	71.84	66.37	72.10	57.33	65.48	66.60	64.78
MARIS (Pr@90)	42.38	43.15	40.69	36.58	38.18	30.42	29.94	32.00	31.29

scores higher than 90%. According to the last row of Tab. 1, our method typically segments a high-quality mask.

Table 2: Performance comparison among each component of MARIS, including Feature Enhancement (FE), Mutual-Aware Attention (MA), and Mask Decoder (DE).

Settings	Methods	Pr@70	Pr@80	Pr@90	IoU
# 1	w/o FE	71.92	64.51	37.84	69.19
# 2	w/o MA	77.28	69.03	39.94	74.32
# 3	w/o DE	78.82	69.69	40.04	74.97
# 4	Ours	80.36	72.11	42.38	76.20

Ablation Study

To verify the effectiveness of the proposed modules of our method, we conduct ablation studies to investigate each component, including Feature Enhancement (FE), Mutual-Aware Attention (MA), and Mask Decoder (DE) on the RefCOCO val dataset, as shown in Tab. 2. Note that we use the SAM's decoder (Kirillov et al. 2023) for the variant excluding the proposed decoder.

Mutual-Aware Attention Blocks Mutual-Aware Attention blocks are introduced to weight different image regions and different words in the sentence. It brings an improvement by 1.88% in terms of IoU score. To verify the superiority of Mutual-Aware Attention, we conduct experiments that use other methods (Kim et al. 2022; Ding et al. 2022; Hu et al. 2020) to incorporate features of different modalities. Specifically, ReSTR (Kim et al. 2022) utilizes a transformer encoder (TE) to model the long-range dependencies. VLT (Ding et al. 2022) adopts the Spatial Dynamic Fusion (SDF) to produce different linguistic feature vectors, which is equivalent to using only Visual-Guided Attention. BRINet (Hu et al. 2020) introduces a serial bidirectional cross-modal (BCM) module to utilize visual and linguistic guidance.

According to Tab. 3, our MA outperforms TE, SDF, BCM by 1.35%, 1.12%, 1.00% IoU score, respectively. This is because existing methods only explore the informative words of each image region, while our method also provides the corresponding image regions of each word in the language

Table 3: The comparison between our MA and other methods, including TE in ReSTR, SDF in VLT, BCM in BRINet, and without attention mask.

Settings	Methods	Pr@70	Pr@80	Pr@90	IoU
# 5	TE (ReSTR)	78.62	70.17	39.77	74.85
# 6	SDF (VLT)	78.91	70.25	40.22	75.08
# 7	BCM (BRINet)	79.17	70.54	40.56	75.20
# 8	w/o attn. mask	80.08	71.62	41.71	75.52
# 4	MA (Ours)	80.36	72.11	42.38	76.20

expression and generates vision-aware linguistic features. We also provide some visualized examples in the supplementary material to show that our method generates a more accurate and high-quality mask than others. Finally, according to # 8, the attention mask alleviates the interference of irrelevant pairs between visual and linguistic features, which further improves the performance by 0.68% IoU.

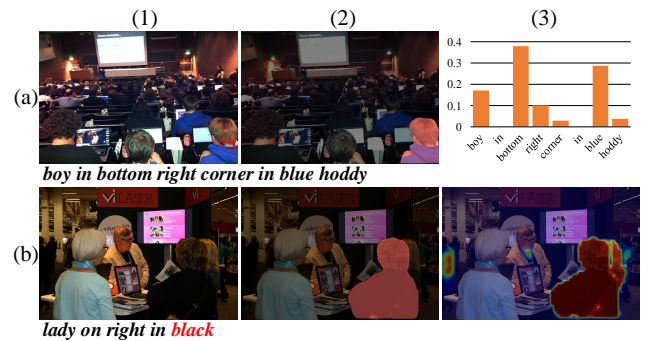


Figure 5: The result of Vision-Guided Attention (a) and Language-Guided Attention (b).

Besides, we visualize the output of Vision-Guided Attention and Language-Guided Attention in Fig. 5(a) and (b), respectively. For the red rectangle in Fig. 5(a1), we list attention weights of each word in Fig. 5(a3). Our model considers 'bottom' and 'blue' as the most informative words. Thus, our prediction mask accurately locates the bottom boy in blue, as shown in Fig. 5(a2). Similarly, for the word 'black', we show its attention map in Fig. 5(b3). In the Mask Decoder,

the final segmentation mask is refined according to the attention map. Our prediction mask is shown in Fig. 5(b2).

Mask Decoder According to Tab. 2, replacing the Mask Decoder with SAM’s decoder reduces the IoU score by 1.23%. This reduction is caused by the *token to image attn.* (TOI-A) layer in SAM’s decoder. Specifically, the TOI-A layer performs cross-attention by taking prompt tokens containing output tokens and linguistic features as queries (Q), visual features as keys (K) and vectors (V). Since these output tokens are initialized randomly, they make an uncertain adjustment to the evolved visual features and thus affect the performance. To verify the disadvantage of TOI-A layer for RIS, we insert this layer into each block of our decoder. As shown in # 9 of Tab. 4, the TOI-A layer leads to 0.80% IoU decrease. Besides, to verify the effectiveness of explicit linguistic guidance (ELP), we also implement the experiment without explicit linguistic guidance (# 10). Similar to VLT (Ding et al. 2022), we multiply F_{val} with F_{lav} to obtain the input feature of the Mask Decoder. # 10 in Tab. 4 indicates that explicit linguistic guidance improves the IoU performance by 1.78%, which demonstrates the effectiveness of the proposed decoder.

Table 4: Ablation study of the Mask Decoder.

Settings	Methods	Pr@70	Pr@80	Pr@90	IoU
# 9	w/ TOI-A	79.21	71.07	40.65	75.40
# 10	w/o ELP	78.55	67.96	38.62	74.42
# 4	Ours	80.36	72.11	42.38	76.20

Feature Enhancement As shown in Tab. 5, the Feature Enhancement module significantly improves the performance of MARIS by 7.01% IoU score. To understand Feature Enhancement comprehensively, we conduct the experiment by using another well-known backbone-adaption baseline. Specifically, we adopt VIT-DET (Li et al. 2022b) as the compared baseline, which uses only the feature map from the last layer of the backbone to generate multi-scale features. The quantitative evaluations are shown in Tab. 5.

Table 5: Ablation study of the Feature Enhancement.

Settings	Methods	Pr@70	Pr@80	Pr@90	IoU
# 1	w/o FE	71.92	64.51	37.84	69.19
# 11	VIT-DET	74.74	66.79	37.85	71.55
# 4	Ours	80.36	72.11	42.38	76.20

Compared with removing Feature Enhancement (FE) module (# 1), multi-scale features generated from the last layer improve the performance by 2.36%. However, compared with using features from different layers, this baseline shrinks the IoU performance by 4.65%. The reason for performance degradation is that features from the last layer contain highly global information, and multi-scale features generated from the last layer exhibit a limited representation of grained details that are essential for RIS.

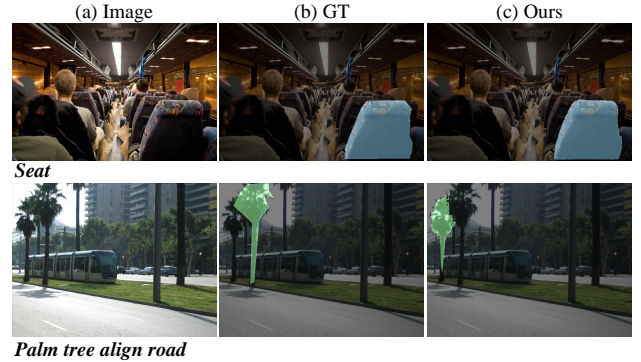


Figure 6: The successful example (top) and failed example (bottom) in PhraseCut.

Generalization Ability

To demonstrate the generalization ability of our method, we conduct experiments on the test split of PhraseCut (Wu et al. 2020). PhraseCut contains 1287 categories, which is much more diverse than 80 categories in COCO. Thus, we compare with two previous methods (as their parameters are available online) on PhraseCut to evaluate their generalization ability.

As shown in Tab. 6, our method surpasses previous methods in terms of generalization ability. For example, when training on the RefCOCO dataset, our method exceeds CRIS and LAVT by 7.29% and 6.14%, respectively. This advantage comes from the frozen text encoder and image encoder and the introduction of Feature Enhancement. In contrast, encoders of other methods are trainable and thus might be biased to the fine-tuned dataset. We also provide some successful and failed visualized examples in Fig. 6.

Table 6: Generalization ability of different methods.

Training Set	IoU results on PhraseCut		
	CRIS	LAVT	Ours
RefCOCO	15.53	16.68	22.82
RefCOCO+	16.30	16.64	21.68
G-Ref	16.24	16.05	22.47

Conclusion

This paper proposes a novel referring image segmentation method called MARIS, which effectively uses mutual-aware attention features and incorporates the powerful knowledge from SAM into RIS. Our model contains three components: the Feature Enhancement module, the Mutual-Aware Attention block, and a Mask Decoder. To be specific, the Feature Enhancement module incorporates global and local features to transfer the knowledge from the frozen image encoder of SAM. Subsequently, the Mutual-Aware Attention block produces language-aware visual features and vision-aware linguistic features by weighting each word of the sentence and each region of visual features. Finally, we design a Mask Decoder to utilize explicit linguistic guidance. Specifically, we introduce the multi-modal query token to integrate

visual and linguistic properties. Extensive experiments on three well-known benchmarks and PhraseCut demonstrate that MARIS achieves new state-of-the-art performance and great generalization ability.

References

- Carion, N.; Massa, F.; Synnaeve, G.; Usunier, N.; Kirillov, A.; and Zagoruyko, S. 2020. End-to-end object detection with transformers. In *European conference on computer vision*, 213–229. Springer.
- Cheng, B.; Misra, I.; Schwing, A. G.; Kirillov, A.; and Girdhar, R. 2022. Masked-attention mask transformer for universal image segmentation. In *Proceedings of the IEEE/CVF Conference on Computer Vision and Pattern Recognition*, 1290–1299.
- Ding, H.; Liu, C.; Wang, S.; and Jiang, X. 2022. Vlt: Vision-language transformer and query generation for referring segmentation. *IEEE Transactions on Pattern Analysis and Machine Intelligence*.
- Dosovitskiy, A.; Beyer, L.; Kolesnikov, A.; Weissenborn, D.; Zhai, X.; Unterthiner, T.; Dehghani, M.; Minderer, M.; Heigold, G.; Gelly, S.; et al. 2020. An image is worth 16x16 words: Transformers for image recognition at scale. *arXiv preprint arXiv:2010.11929*.
- Gu, X.; Lin, T.-Y.; Kuo, W.; and Cui, Y. 2021. Open-vocabulary object detection via vision and language knowledge distillation. *arXiv preprint arXiv:2104.13921*.
- He, K.; Gkioxari, G.; Dollár, P.; and Girshick, R. 2017. Mask r-cnn. In *Proceedings of the IEEE international conference on computer vision*, 2961–2969.
- Hu, R.; Rohrbach, M.; and Darrell, T. 2016. Segmentation from natural language expressions. In *Computer Vision—ECCV 2016: 14th European Conference, Amsterdam, The Netherlands, October 11–14, 2016, Proceedings, Part I 14*, 108–124. Springer.
- Hu, Z.; Feng, G.; Sun, J.; Zhang, L.; and Lu, H. 2020. Bi-directional relationship inferring network for referring image segmentation. In *Proceedings of the IEEE/CVF conference on computer vision and pattern recognition*, 4424–4433.
- Jing, Y.; Kong, T.; Wang, W.; Wang, L.; Li, L.; and Tan, T. 2021. Locate then segment: A strong pipeline for referring image segmentation. In *Proceedings of the IEEE/CVF Conference on Computer Vision and Pattern Recognition*, 9858–9867.
- Kazemzadeh, S.; Ordonez, V.; Matten, M.; and Berg, T. 2014. Referitgame: Referring to objects in photographs of natural scenes. In *Proceedings of the 2014 conference on empirical methods in natural language processing (EMNLP)*, 787–798.
- Kim, N.; Kim, D.; Lan, C.; Zeng, W.; and Kwak, S. 2022. Restr: Convolution-free referring image segmentation using transformers. In *Proceedings of the IEEE/CVF Conference on Computer Vision and Pattern Recognition*, 18145–18154.
- Kirillov, A.; Mintun, E.; Ravi, N.; Mao, H.; Rolland, C.; Gustafson, L.; Xiao, T.; Whitehead, S.; Berg, A. C.; Lo, W.-Y.; et al. 2023. Segment anything. *arXiv preprint arXiv:2304.02643*.
- Li, J.; Li, D.; Savarese, S.; and Hoi, S. 2023. Blip-2: Bootstrapping language-image pre-training with frozen image encoders and large language models. *arXiv preprint arXiv:2301.12597*.
- Li, J.; Selvaraju, R.; Gotmare, A.; Joty, S.; Xiong, C.; and Hoi, S. C. H. 2021. Align before fuse: Vision and language representation learning with momentum distillation. *Advances in neural information processing systems*, 34: 9694–9705.
- Li, L. H.; Zhang, P.; Zhang, H.; Yang, J.; Li, C.; Zhong, Y.; Wang, L.; Yuan, L.; Zhang, L.; Hwang, J.-N.; et al. 2022a. Grounded language-image pre-training. In *Proceedings of the IEEE/CVF Conference on Computer Vision and Pattern Recognition*, 10965–10975.
- Li, W.; Gao, C.; Niu, G.; Xiao, X.; Liu, H.; Liu, J.; Wu, H.; and Wang, H. 2020. Unimo: Towards unified-modal understanding and generation via cross-modal contrastive learning. *arXiv preprint arXiv:2012.15409*.
- Li, Y.; Mao, H.; Girshick, R.; and He, K. 2022b. Exploring plain vision transformer backbones for object detection. In *European Conference on Computer Vision*, 280–296. Springer.
- Lin, T.-Y.; Goyal, P.; Girshick, R.; He, K.; and Dollár, P. 2017. Focal loss for dense object detection. In *Proceedings of the IEEE international conference on computer vision*, 2980–2988.
- Lin, T.-Y.; Maire, M.; Belongie, S.; Hays, J.; Perona, P.; Ramanan, D.; Dollár, P.; and Zitnick, C. L. 2014. Microsoft coco: Common objects in context. In *Computer Vision—ECCV 2014: 13th European Conference, Zurich, Switzerland, September 6–12, 2014, Proceedings, Part V 13*, 740–755. Springer.
- Liu, C.; Ding, H.; and Jiang, X. 2023. GRES: Generalized referring expression segmentation. In *Proceedings of the IEEE/CVF Conference on Computer Vision and Pattern Recognition*, 23592–23601.
- Liu, C.; Lin, Z.; Shen, X.; Yang, J.; Lu, X.; and Yuille, A. 2017. Recurrent multimodal interaction for referring image segmentation. In *Proceedings of the IEEE international conference on computer vision*, 1271–1280.
- Liu, D.; Zhang, H.; Wu, F.; and Zha, Z.-J. 2019. Learning to assemble neural module tree networks for visual grounding. In *Proceedings of the IEEE/CVF International Conference on Computer Vision*, 4673–4682.
- Liu, Z.; Lin, Y.; Cao, Y.; Hu, H.; Wei, Y.; Zhang, Z.; Lin, S.; and Guo, B. 2021. Swin transformer: Hierarchical vision transformer using shifted windows. In *Proceedings of the IEEE/CVF international conference on computer vision*, 10012–10022.
- Luo, G.; Zhou, Y.; Sun, X.; Cao, L.; Wu, C.; Deng, C.; and Ji, R. 2020. Multi-task collaborative network for joint referring expression comprehension and segmentation. In *Proceedings of the IEEE/CVF Conference on computer vision and pattern recognition*, 10034–10043.

- Mao, J.; Huang, J.; Toshev, A.; Camburu, O.; Yuille, A. L.; and Murphy, K. 2016. Generation and comprehension of unambiguous object descriptions. In *Proceedings of the IEEE conference on computer vision and pattern recognition*, 11–20.
- Milletari, F.; Navab, N.; and Ahmadi, S.-A. 2016. V-net: Fully convolutional neural networks for volumetric medical image segmentation. In *2016 fourth international conference on 3D vision (3DV)*, 565–571. Ieee.
- Radford, A.; Kim, J. W.; Hallacy, C.; Ramesh, A.; Goh, G.; Agarwal, S.; Sastry, G.; Askell, A.; Mishkin, P.; Clark, J.; et al. 2021. Learning transferable visual models from natural language supervision. In *International conference on machine learning*, 8748–8763. PMLR.
- Shi, H.; Li, H.; Meng, F.; and Wu, Q. 2018. Key-word-aware network for referring expression image segmentation. In *Proceedings of the European Conference on Computer Vision (ECCV)*, 38–54.
- Toneva, M.; Sordoni, A.; Combes, R. T. d.; Trischler, A.; Bengio, Y.; and Gordon, G. J. 2018. An empirical study of example forgetting during deep neural network learning. *arXiv preprint arXiv:1812.05159*.
- Vaswani, A.; Shazeer, N.; Parmar, N.; Uszkoreit, J.; Jones, L.; Gomez, A. N.; Kaiser, Ł.; and Polosukhin, I. 2017. Attention is all you need. *Advances in neural information processing systems*, 30.
- Wang, X.; Girshick, R.; Gupta, A.; and He, K. 2018. Non-local neural networks. In *Proceedings of the IEEE conference on computer vision and pattern recognition*, 7794–7803.
- Wang, Z.; Lu, Y.; Li, Q.; Tao, X.; Guo, Y.; Gong, M.; and Liu, T. 2022. Cris: Clip-driven referring image segmentation. In *Proceedings of the IEEE/CVF conference on computer vision and pattern recognition*, 11686–11695.
- Wu, C.; Lin, Z.; Cohen, S.; Bui, T.; and Maji, S. 2020. Phrasecut: Language-based image segmentation in the wild. In *Proceedings of the IEEE/CVF Conference on Computer Vision and Pattern Recognition*, 10216–10225.
- Xu, J.; De Mello, S.; Liu, S.; Byeon, W.; Breuel, T.; Kautz, J.; and Wang, X. 2022. Groupvit: Semantic segmentation emerges from text supervision. In *Proceedings of the IEEE/CVF Conference on Computer Vision and Pattern Recognition*, 18134–18144.
- Xu, L.; Huang, M. H.; Shang, X.; Yuan, Z.; Sun, Y.; and Liu, J. 2023. Meta compositional referring expression segmentation. In *Proceedings of the IEEE/CVF Conference on Computer Vision and Pattern Recognition*, 19478–19487.
- Yang, X.; Li, Z.; Xu, H.; Zhang, H.; Ye, Q.; Li, C.; Yan, M.; Zhang, Y.; Huang, F.; and Huang, S. 2023. Learning Trajectory-Word Alignments for Video-Language Tasks. *arXiv preprint arXiv:2301.01953*.
- Yang, Z.; Wang, J.; Tang, Y.; Chen, K.; Zhao, H.; and Torr, P. H. 2022. Lavt: Language-aware vision transformer for referring image segmentation. In *Proceedings of the IEEE/CVF Conference on Computer Vision and Pattern Recognition*, 18155–18165.
- Ye, L.; Rochan, M.; Liu, Z.; and Wang, Y. 2019. Cross-modal self-attention network for referring image segmentation. In *Proceedings of the IEEE/CVF conference on computer vision and pattern recognition*, 10502–10511.
- Yu, L.; Lin, Z.; Shen, X.; Yang, J.; Lu, X.; Bansal, M.; and Berg, T. L. 2018. MATTNet: Modular attention network for referring expression comprehension. In *Proceedings of the IEEE conference on computer vision and pattern recognition*, 1307–1315.
- Yu, L.; Poirson, P.; Yang, S.; Berg, A. C.; and Berg, T. L. 2016. Modeling context in referring expressions. In *Computer Vision—ECCV 2016: 14th European Conference, Amsterdam, The Netherlands, October 11–14, 2016, Proceedings, Part II 14*, 69–85. Springer.
- Zhou, L.; Palangi, H.; Zhang, L.; Hu, H.; Corso, J.; and Gao, J. 2020. Unified vision-language pre-training for image captioning and vqa. In *Proceedings of the AAAI conference on artificial intelligence*, volume 34, 13041–13049.